RAPID COMMUNICATIONS

PHYSICAL REVIEW B VOLUME 45, NUMBER 21 1 JUNE 1992-I

New ground states in unconventional superconductors: Broken translational and time-reversal symmetry

Mario Palumbo and Paul Muzikar
Department of Physics, Purdue University, West Lafayette, Indiana 47907
(Received 21 October 1991; revised manuscript received 10 April 1992)

We explore the spatial structure of novel ground states which can arise in unconventional superconductors. If the coefficients in the Ginzburg-Landau functional are in the appropriate range, the free energy, even in zero applied field, is minimized by a state with a spatially varying order parameter. This variation leads to supercurrents, which generate substantial magnetic fields. The interactions between the vector potential and the order parameter are responsible for the net lowering of the free energy. We use a simulated annealing technique to find numerically the minima of the Ginzburg-Landau functional.

I. INTRODUCTION

The variety of superconducting compounds discovered in recent years has stimulated much interest in the theory of unconventional superconductors.[1-3] In particular, there is strong evidence that the order parameter in heavy-fermion materials, such as UPt_3, is unconventional.[4,5] By unconventional, we mean that the energy gap $\Delta(\hat{\mathbf{k}})$ has less rotational symmetry than the normal-state crystal.[6] In a previous paper[7] we discovered that the spatially homogeneous, zero-applied-magnetic-field state of such a superconductor can be unstable in the following sense: The free energy can be lowered by a spatially varying distortion of the order parameter which generates supercurrents and a magnetic field. Thus the equilibrium state of such an unconventional superconductor will be a complicated affair, in which the system generates its own magnetic field, and in which the spatial variations of the order parameter and field are intricately coupled. Translational and time-reversal symmetry are broken.

The stability analysis in Ref. 7 did not allow us to study the fully developed new equilibrium state; we could (1) show the uniform state was unstable when the coefficients in the Ginzburg-Landau (GL) functional satisfied certain conditions, and (2) determine the form of the unstable mode. So in this paper we report the results of a numerical minimization of the GL functional; we chose the coefficients in the GL functional to be in the unstable range. To do the calculations we used the method of simulated annealing which has recently been shown to be useful in attacking GL problems in superconductivity.[8]

As in Ref. 7, we studied an order parameter transforming according to the two-dimensional E_{1g} representation of the point group D_{6h}. The order parameter is a complex two-dimensional vector, $\boldsymbol{\eta}$, transforming as a vector in the xy plane. Note that the GL theory for the E_{1u} representation is identical, so our considerations cover this case as well. We consider a situation in which the order parameter and magnetic field are functions of x and y but are independent of z. The magnetic field, $\mathbf{h}(\mathbf{r})$, has only a z component, which we call h.

II. CALCULATIONAL METHOD

The GL free-energy density is given by[7,9,10]

$$f=-\alpha|\boldsymbol{\eta}|^2+\beta_1|\boldsymbol{\eta}|^4+\beta_2|\boldsymbol{\eta}\cdot\boldsymbol{\eta}|^2+K_1D_i\eta_jD_i^*\eta_j^*+K_2D_i\eta_iD_j^*\eta_j^*+K_3D_i\eta_jD_j^*\eta_i^*+h^2/8\pi. \quad (1)$$

Here, the gauge-invariant derivative is defined by $D_j=\partial_j-(2ie/\hbar c)A_j$. We define a correlation length ξ in the following way:[11]

$$\xi=(K_{123}/\alpha)^{1/2}. \quad (2)$$

It is then convenient to define a dimensionless order parameter, length scale, vector potential, magnetic field, and free energy in the following way:

$$\tilde{\eta}_j=(2\beta_{12}/\alpha)^{1/2}\eta_j, \quad (3)$$

$$\tilde{r}_j=r_j/\xi, \quad (4)$$

$$\tilde{A}_j=(2e\xi/\hbar c)A_j, \quad (5)$$

$$\tilde{h}_j=(2e\xi^2/\hbar c)h_j, \quad (6)$$

$$\tilde{f}=(2\beta_{12}/\alpha^2)f. \quad (7)$$

In terms of these dimensionless variables we then have

$$\tilde{f}=-\tilde{\eta}_j\tilde{\eta}_j^*+1/2\tilde{\beta}_1(\tilde{\eta}_j\tilde{\eta}_j^*)^2+1/2\tilde{\beta}_2|\tilde{\eta}_j\tilde{\eta}_j|^2+\tilde{K}_1\tilde{D}_i\tilde{\eta}_j\tilde{D}_i^*\tilde{\eta}_j^*+\tilde{K}_2\tilde{D}_i\tilde{\eta}_i\tilde{D}_j^*\tilde{\eta}_j^*+\tilde{K}_3\tilde{D}_i\tilde{\eta}_j\tilde{D}_j^*\tilde{\eta}_i^*+\kappa^2\tilde{h}^2. \quad (8)$$

Here, we have $\tilde{\beta}_i=\beta_i/\beta_{12}$, $\tilde{K}_i=K_i/K_{123}$, and $\kappa^2=\beta_{12}h^2c^2/16\pi e^2K_{123}^2$.

The basic task is then to find the functions $\tilde{\eta}_j(\tilde{r}_i)$ and $\tilde{A}_j(\tilde{r}_i)$ which minimize the following quantity:

$$\tilde{F}=\frac{1}{\tilde{L}_x\tilde{L}_y}\int d^2\tilde{r}\,\tilde{f}=\frac{2\beta_{12}}{\alpha^2L_xL_y}\int d^2r f, \quad (9)$$

subject to the appropriate boundary conditions. Here we have normalized the free energies by the area, $L_xL_y=\tilde{L}_x\tilde{L}_y\xi^2$, so that we can directly compare the $\tilde{F}$'s arising from different runs with different areas.

To carry out this minimization we use the simulated an-

nealing technique developed by Doria, Gubernatis, and Rainer (DGR). We discretize (9), and replace the derivatives by gauge-invariant differences in a manner analogous to DGR. We then carry out the simulated annealing procedure exactly as described in DGR; this procedure is discussed in great detail in Corana *et al.*[12] We continually update our step sizes so that a reasonable number of random moves are accepted.

The boundary conditions are set to insure that the total magnetic flux in the system is equal to a given number of flux quanta:[8]

$$\mathbf{A}(\mathbf{r}+L_x\hat{\mathbf{x}})=\mathbf{A}(\mathbf{r}), \tag{10}$$

$$\mathbf{A}(\mathbf{r}+L_y\hat{\mathbf{y}})=\mathbf{A}(\mathbf{r})-BL_y\hat{\mathbf{x}}, \tag{11}$$

$$\eta(\mathbf{r}+L_x\hat{\mathbf{x}})=\eta(\mathbf{r}), \tag{12}$$

$$\eta(\mathbf{r}+L_y\hat{\mathbf{y}})=\eta(\mathbf{r})\exp(-2ieBL_yx/\hbar c). \tag{13}$$

Hence, we are minimizing F at fixed $B=\langle h\rangle=N\phi_0/L_xL_y$, where the brackets indicate a spatial average and ϕ_0 is the superconducting flux quantum. In all the results shown here we choose $\beta_2<0$, so that in the absence of the instability the order parameter would be of the form $\eta\sim(1,0)$, up to a rotation and a phase factor. In this paper we display results for the following set of coefficients: $\tilde{\beta}_1=1.5$, $\tilde{\beta}_2=-0.5$, $\tilde{K}_1=0.5$, $\tilde{K}_2=15.0$, $\tilde{K}_3=-14.5$, and $\kappa=12.0$. This set puts us in the unstable range, as can be verified from Eqs. (14)–(18) of Ref. 7. Note that in the unperturbed (1,0) state we have $\tilde{F}=-0.5$.

III. $B=0$ RESULTS

In this section we fix the boundary conditions so that $B=\langle h\rangle=0$. This means that the order parameter and vector potential are simply forced to obey periodic boundary conditions across our system. Figure 1 shows plots of the magnetic field and order parameter for the choice of GL coefficients mentioned in the previous section.

The salient features are as follows: (1) All the physical quantities oscillate with a fundamental wavelength quite close to that predicted by the stability analysis. (2) The deviations of the order parameter from the unperturbed (1,0) state are quite significant, as is evident from the large fluctuations in the quantity $|\tilde{\eta}_j\tilde{\eta}_j|$. (3) We are measuring $\tilde{h}$ in units comparable to H_{c2} [see Eq. (6)], so that the maximum values attained are quite large, being of the order 0.06. (4) For the free energy we have $\tilde{F}=-0.567$, a value markedly lower than the unperturbed state's value of $\tilde{F}=-0.5$.

The wavelength of the instability, Λ, can be computed from Eq. (16) of Ref. 7. In rescaled units we get

$$\tilde{\Lambda}=\Lambda/\xi=\pi(8\beta_{12}\kappa^2/|\beta_2|)^{1/4}. \tag{14}$$

For our parameters this yields

$$\tilde{\Lambda}=\sqrt{48}\pi\approx 21.8. \tag{15}$$

From Figure 1 we can see that the actual wavelength is about 25; this is in reasonably good agreement with the above estimate, since nonlinear effects which stabilize the pattern are not included in the calculation of Λ. In addition, the wavelength in the data may deviate from its ideal value in order to fit in the finite-sized box.

We note that $|\tilde{\eta}_j\tilde{\eta}_j|$ attains values as low as 0.0015, while the minimum value of $\eta_j\eta_j^*$ is about 0.893; at these places the order parameter is very nearly in the $(1,i)$ state, even though the coefficient β_2 is negative.

Experience with many simulated annealing runs has shown us that most runs produce a somewhat disordered pattern as in Fig. 1. The result is influenced by the geometry of the situation, i.e., our choice of L_x and L_y,

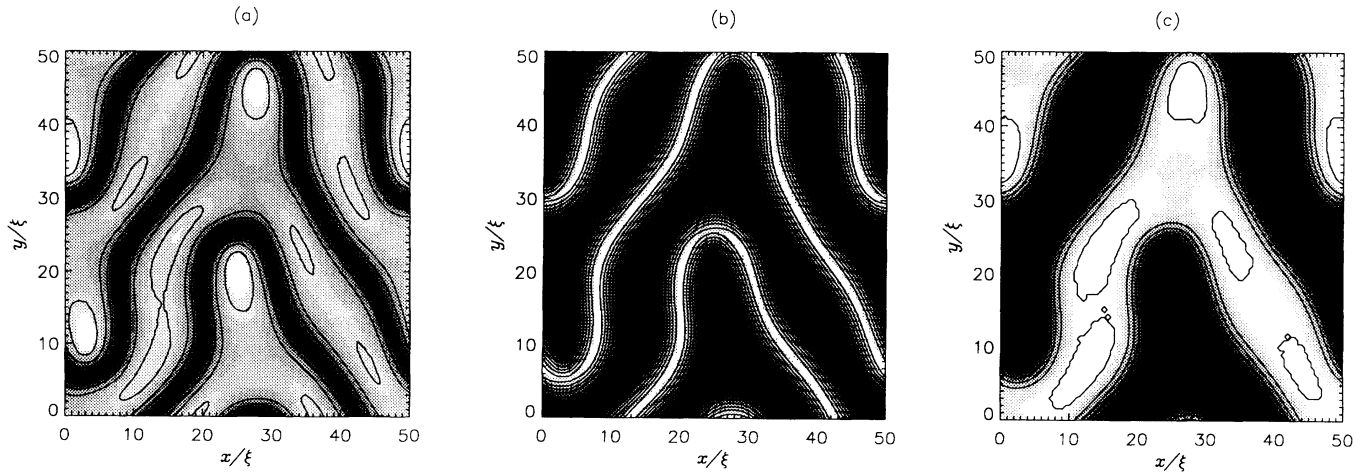

FIG. 1. Results from a $B=0$ simulated annealing run, with the parameters listed in Sec. II. The lattice was discretized in units of 0.5ξ. (a) Contour plot of $\tilde{\eta}_j\tilde{\eta}_j^*$. The lightest regions have values of approximately 1.26, while the darkest regions have values of about 0.893. (b) Contour plot of $|\tilde{\eta}_j\tilde{\eta}_j|$. The lightest regions have values of about 0.964, while the darkest have values of about 0.0015. (c) Contour plot of the scaled magnetic field, $\tilde{h}$. The lightest regions have values of about 0.064, and the darkest regions have values of approximately -0.064.

and their relation to the preferred wavelength of the pattern. The free energy is always in the vicinity of $\tilde{F} = -0.56$.

IV. $B \neq 0$ RESULTS

We performed simulated annealing runs with the same set of parameters as in the previous section, but adjusted the boundary conditions to fix $\langle h \rangle$, or N, the number of flux quanta, at various values. In this section all runs have $\tilde{L}_x = 40$ and $\tilde{L}_y = 40$, so that $B = N\phi_0/1600\xi^2$. In Fig. 2 we plot the free energy $\tilde{F}$, and the field $H = 4\pi\partial\langle f \rangle/\partial B$ as functions of N. To evaluate H we use the virial theorem recently introduced by Doria, Gubernatis, and Rainer.[13] The results are quite striking. To good precision, $\tilde{F}$ is constant out to about $N = 14$, and then starts to rise. In agreement with this, when we compute H via the virial theorem we find that it is zero to good accuracy out to $N = 14$, and then starts to rise. Figure 3 shows a typical result for $N = 4$, while Fig. 4 shows a result for $N = 18$.

Our preliminary interpretation is as follows. Between $N = 0$ and about $N = 14$ the system is in a two-phase state; part of the superconductor is occupied by the strips, and part by vortices. The strips are similar to the modulations that appear in the $B = 0$ case, and usually close in on themselves as in Fig. 3. The vortices are smaller objects, at the center of which the magnetic field reaches a local minimum. The phase of the order parameter changes by 2π on a contour which encloses one of the vortices. Thus, the vortices are singular, and η_x and η_y must vanish somewhere in the core region.

As N increases the number of vortices increases, and the area of the system covered by the strips decreases. Past $N = 14$, or $B = 7\phi_0/800\xi^2$, the strips have disappeared. We note that at $N = 14$ the separation between nearest-neighbor vortices is approximately $\tilde{\Lambda}/2$. We also note that the vortices change their symmetry at $N = 14$; for $N < 14$ they have a triangular symmetry, while for $N > 14$ they have a circular symmetry. It may be possible to interpret an array of these vortices as a domain, and the strips as the result of a combination of vortices and antivortices. For a discussion of unusual vortices when the GL coefficients are in the stable range see Refs. 14 and 15.

We can understand why the magnetic field at the center of the vortices goes down, as is seen in Figs. 3 and 4, from

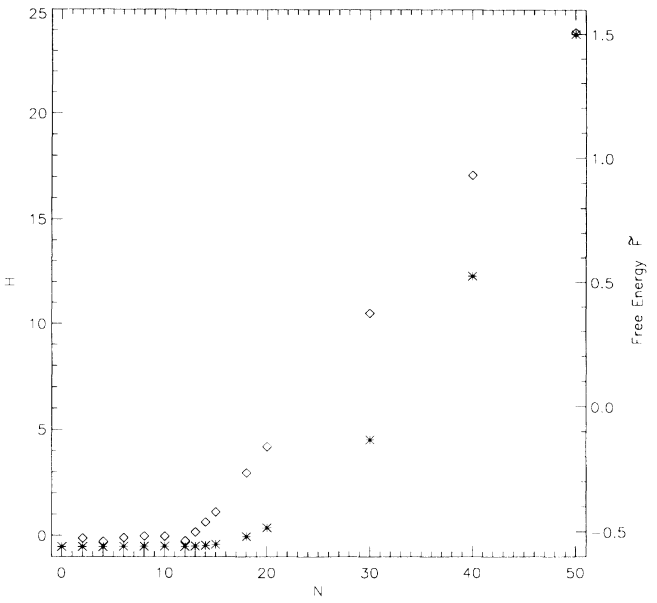

FIG. 2. Results from a succession of runs, with the parameters given in Sec. II, for various values of the total magnetic flux through the system. The scaled free energy, $\tilde{F}$, represented by the asterisks, is defined in Sec. II; N is the number of flux quanta, so that $B = N\phi_0/1600\xi^2$. H, represented by the diamonds, is measured in units of $\phi_0/1600\xi^2$.

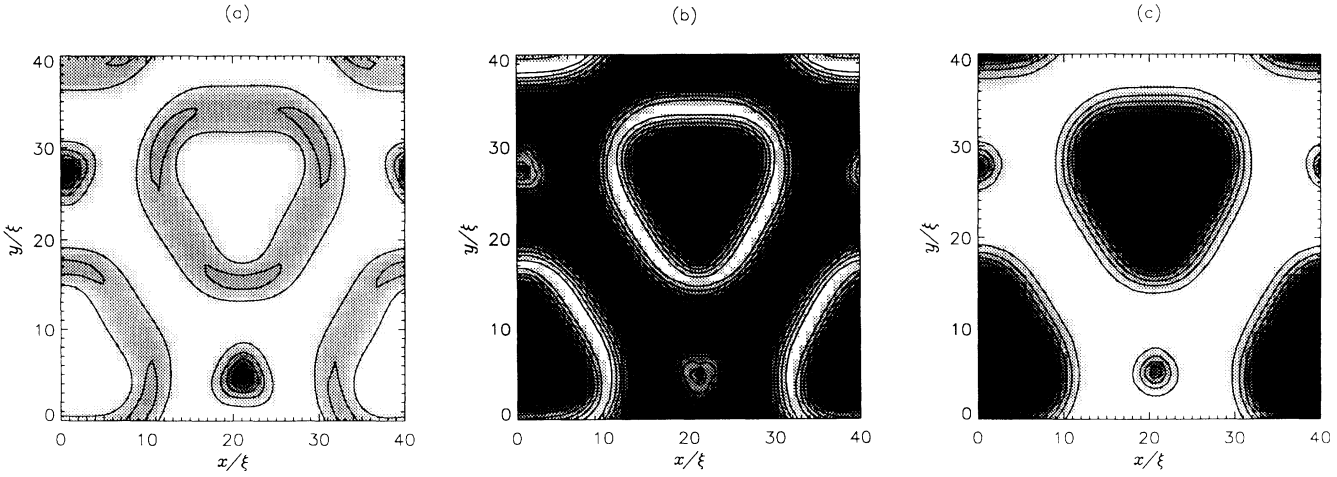

FIG. 3. Results from an $N = 4$ run, so that $B = \phi_0/400\xi^2$. The parameters are given in Sec. II; the lattice was discretized in units of 0.8ξ. (a) Contour plot of $\tilde{\eta}_j\tilde{\eta}_j^*$. The lightest regions have values of about 1.22, while the darkest regions descend to values of 0.427. (b) Contour plot of $|\tilde{\eta}_j\tilde{\eta}_j|$. The lightest regions have values of 0.98, and the darkest have values of 0.00. (c) Contour plot of the scaled magnetic field, $\tilde{h}$. The lightest regions have values of 0.0579, and the darkest have values of -0.0588.

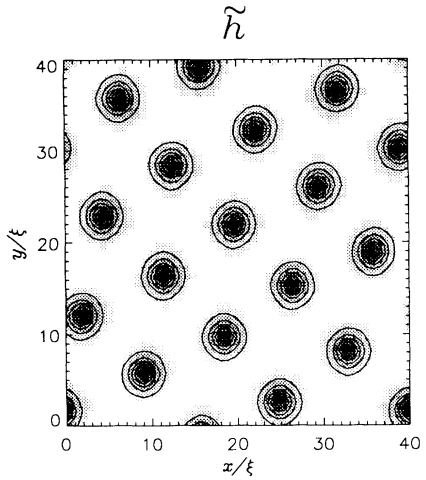

FIG. 4. Results from an $N=18$ run, so that $B=9\phi_0/800\xi^2$. The lattice was discretized in units of 0.8ξ. The parameters are the same as in Fig. 3. We show a contour plot of the scaled magnetic field, $\tilde{h}$. The lightest regions have values of 0.08, while the darkest have values of about 0.003.

the following considerations. Recall that the supercurrent is given by the following expression:

$$J_k = -\frac{4e}{\hbar}\,\mathrm{Im}[K_1\eta_j D_k^*\eta_j^* + \tfrac{1}{2}K_{23}(\eta_k D_j^*\eta_j^* + \eta_j D_j^*\eta_k^*)] + \frac{ie}{\hbar}(K_2-K_3)[\nabla\times(\boldsymbol{\eta}\times\boldsymbol{\eta}^*)]_k\,. \tag{16}$$

Note that with our choice of parameters, the last term has a large coefficient, since K_2 and K_3 are much larger than K_1 and have opposite signs. We have evaluated the current for the configurations shown in Figs. 3 and 4, and indeed the last term makes the dominant contribution.

When the order parameter is of the form $\boldsymbol{\eta}=\eta(\mathbf{R})(1,i)$, this last term produces a current proportional to $\hat{\mathbf{z}}\times\nabla\eta^2$. In the vortex cores, where the magnitude of the order parameter is strongly varying, this term in the current circulates in a counterclockwise direction, reducing h from its value far from the core. We stress that intuition gained from a knowledge of conventional vortices is not applicable in cases where the supercurrent is dominated by the third term in (16).

Since $B > H$, we do not have diamagnetism; the average interior magnetic field is larger than the applied field. In a case as in Fig. 4, for example, surface supercurrents generate a field parallel to the applied field, while the vortices generate a local field in the opposite direction. A discussion of the possibility of unusual magnetic phenomena in unconventional superconductors can be found in the article by Gorkov.[1]

V. DISCUSSION

From a theoretical point of view these novel ground states are quite interesting: The gauge-invariant coupling of the order parameter to the vector potential induces an intricately patterned equilibrium state. From an experimental viewpoint we note that the coefficients K_i and β_i can be varied by adding impurities and by varying external parameters such as the pressure. Hence, in any existing unconventional superconductors, the coefficients in the GL functional could be tuned in an attempt to reach the unstable region.

ACKNOWLEDGMENTS

This work was supported by the National Science Foundation under Grant No. DMR88-09854 through the Science and Technology Center for Superconductivity. We thank Jim Sauls for many useful conversations. One of us (M.P.) is grateful to J. Gubernatis for arranging a visit to Los Alamos National Laboratory, and is especially grateful to Luc Daemen for much assistance in doing computations on the Los Alamos facilities.

[1] L. P. Gorkov, Sov. Sci. Rev., Sect. A **9**, 1 (1987).
[2] J. F. Annett, N. Goldenfeld, and S. R. Renn, in *Physical Properties of High Temperature Superconductors II*, edited by D. M. Ginsberg (World Scientific, Singapore, 1990), Chap. 9.
[3] J. F. Annett, Adv. Phys. **39**, 83 (1990).
[4] C. H. Choi and J. A. Sauls, Phys. Rev. Lett. **66**, 484 (1991).
[5] S. Adenwalla, S. W. Lin, Q. Z. Ran, Z. Zhao, J. B. Ketterson, J. A. Sauls, L. Taillefer, D. G. Hinks, M. Levy, and B. K. Sarma, Phys. Rev. Lett. **65**, 2298 (1990).
[6] D. Rainer, Phys. Scr. **T23**, 106 (1988).
[7] M. Palumbo, P. Muzikar, and J. A. Sauls, Phys. Rev. B **42**, 2681 (1990).
[8] M. M. Doria, J. E. Gubernatis, and D. Rainer, Phys. Rev. B **41**, 6335 (1990).
[9] C. H. Choi and P. Muzikar, Phys. Rev. B **40**, 5144 (1989).
[10] M. Palumbo, C. H. Choi, and P. Muzikar, Physica B **165&166**, 1095 (1990).
[11] We use the notation $K_{123}=K_1+K_2+K_3$, and $\beta_{12}=\beta_1+\beta_2$.
[12] A. Corana, M. Marchesi, C. Martini, and S. Ridella, ACM Trans. Math. Software **13**, 262 (1987).
[13] M. M. Doria, J. E. Gubernatis, and D. Rainer, Phys. Rev. B **39**, 9573 (1989).
[14] T. A. Tokuyasu, D. W. Hess, and J. A. Sauls, Phys. Rev. B **41**, 8891 (1990).
[15] T. A. Tokuyasu and J. A. Sauls, Physica B **165&166**, 347 (1990).

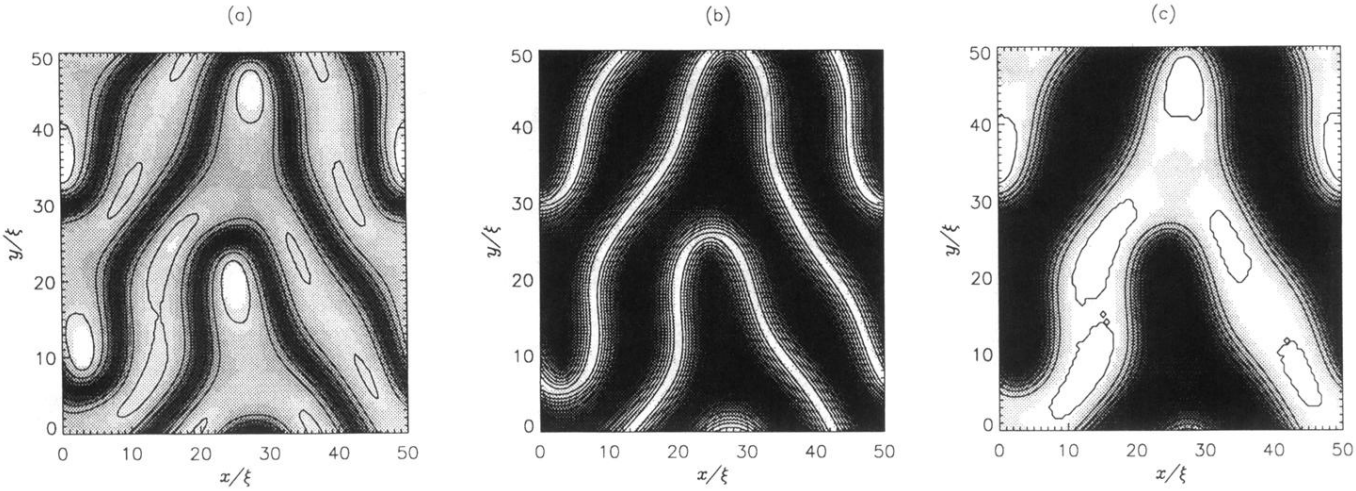

FIG. 1. Results from a $B=0$ simulated annealing run, with the parameters listed in Sec. II. The lattice was discretized in units of 0.5ξ. (a) Contour plot of $\tilde{\eta}_j \tilde{\eta}_j^*$. The lightest regions have values of approximately 1.26, while the darkest regions have values of about 0.893. (b) Contour plot of $|\tilde{\eta}_j \tilde{\eta}_j|$. The lightest regions have values of about 0.964, while the darkest have values of about 0.0015. (c) Contour plot of the scaled magnetic field, $\tilde{h}$. The lightest regions have values of about 0.064, and the darkest regions have values of approximately -0.064.

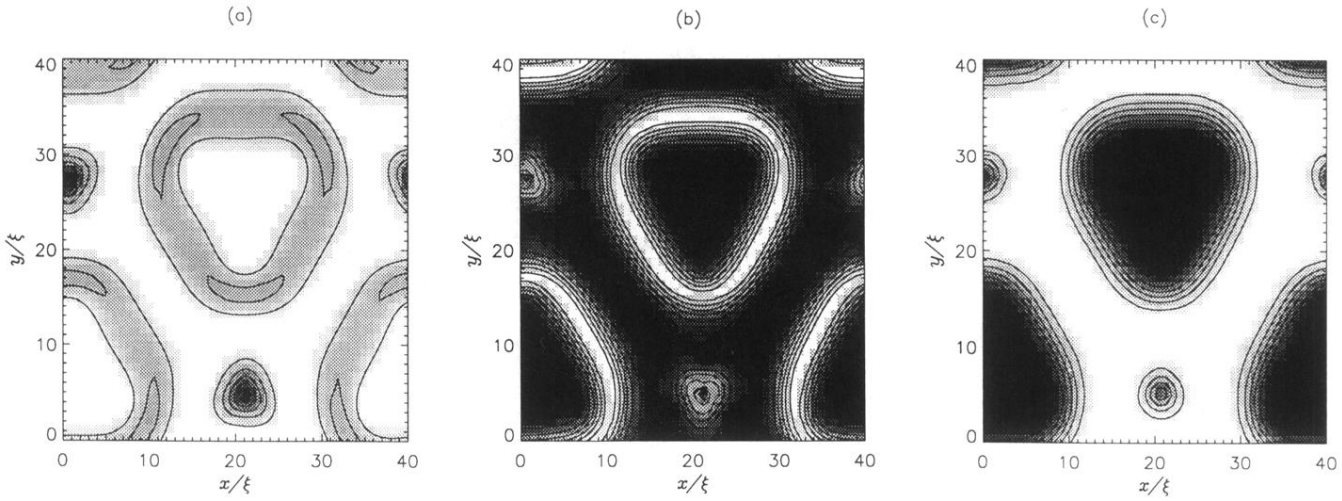

FIG. 3. Results from an $N=4$ run, so that $B=\phi_0/400\xi^2$. The parameters are given in Sec. II; the lattice was discretized in units of 0.8ξ. (a) Contour plot of $\tilde{\eta}_j\tilde{\eta}_j^*$. The lightest regions have values of about 1.22, while the darkest regions descend to values of 0.427. (b) Contour plot of $|\tilde{\eta}_j\tilde{\eta}_j|$. The lightest regions have values of 0.98, and the darkest have values of 0.00. (c) Contour plot of the scaled magnetic field, $\tilde{h}$. The lightest regions have values of 0.0579, and the darkest have values of -0.0588.

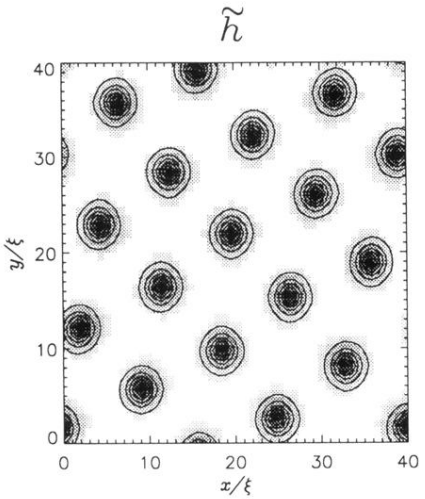

FIG. 4. Results from an $N=18$ run, so that $B=9\phi_0/800\xi^2$. The lattice was discretized in units of 0.8ξ. The parameters are the same as in Fig. 3. We show a contour plot of the scaled magnetic field, $\tilde{h}$. The lightest regions have values of 0.08, while the darkest have values of about 0.003.